Application of optical tweezers in protein folding studies

Master thesis by Laurens Kooijman
Molecular and Cellular Life Science, Utecht University

Supervised by: David-Paul Minde & Sander Tans
2nd superviser: Ineke Braakman

Abstract

Force spectroscopy has proven to be a very promising tool in the protein folding field. With multiple setups and methods to exert force it has been applied in numerous folding studies. This review will focus on the optical tweezers setup and will outline the basics of optical trapping and how it was used before force spectroscopy. The different methods for exerting force and how they are used to obtain information on the energy landscape of protein folding will also be discussed. Finally several studies in which optical tweezers are used to investigate protein folding will be described, including the effect of ribosomes and chaperones on folding and how force is used in biological processes as blood clotting and proteolysis.

Introduction

In the protein folding field the determination of the energy landscape of folding is one of the main approaches. For decades these landscapes have been determined with techniques that measure the protein in bulk. However, with the rise of force spectroscopy a unique insight into the folding process could be obtained. Instead of destabilizing protein with denaturant or a change in temperature, a force is applied with which the unfolding of single proteins is observed. This allows for the observation of millisecond time scale dynamics and intermediate folding states that were previously hidden in the averaging of the ensemble measurements.
Here, we will review the optical tweezer technique, which uses focused laser light to hold and measure the force on micron sized beads. Examples of data and their analysis will be shown, as well as how the data can be used to determine the energy landscape of folding. Additionally we will give some examples of protein folding studies in which optical tweezers have played a pivotal role.

Chapter 1

Optical tweezers, from the principle of optical trapping to unfolding of proteins

1.1 Optical trapping in biology

1.1.1 Principle of optical trapping

The principle of optical trapping is the reflection and refraction by micron sized objects or cells in a laser beam. Due to the conservation of momentum, the change in direction of the laser beam generates a force on the object [1], [2]. The forces perpendicular to the laser beam keep the object in its center and the forces parallel to the laser beam push or pull the object [3]. Initially two oppositely directed laser beams were used to trap objects, but a single laser beam is sufficient when a high numerical aperture objective and the right material are used [4]. The strength of the optical trap is proportional to the laser intensity and wavelength, object size and the refractive index of the solvent and trapped object [5]–[7]. The generation of force by the laser beam and the optical trap has been thoroughly reviewed in [8]–[10]. The uses for optical trapping and manipulation that were initially proposed were only in the field of physics. For example the manipulation of single molecules and optical cooling, which have been realized recently [11]–[13].

1.1.2 Optical trapping of cells

In biochemistry and biophysics, optical trapping has taken a great flight which started with the trapping of cells and organelles [14]. For example, after fixing the flagellum of a bacterium to a glass plate, the optical trap was used to turn the cell around its flagellum axis. The recovery to the original position was observed and gave insight into the mechanism of flagellum movement [15]. In the early 90s the optical trap was used to hold mitochondria while they were transported over microtubules in vitro. It was shown that the transport can proceed either way on the microtubule after release from the optical trap. It was also possible to estimate the force of a single dynein motor protein by lowering the laser power until the mitochondria escaped the optical trap [16]. In recent studies the optical trapping of cells has been used to asses the mobility of spermatozoa in various media [17] and trap red blood cells in vivo that would enable non-invasive micro operation in the future [18]. The advancements in the trapping of cells and more applications, e.g. cell stretching, directed growth, are reviewed in [19].

1.1.3 Motor proteins

For the characterization of the movement and forces of single motor proteins, the optical trap was used with protein covered beads. By keeping a bead trapped while the motor proteins on the bead pulled it over a microtubule, the exact deviation from the center of the trap could be determined [20], [21]. The force needed for a certain deviation was calibrated using a solvent flow and the Stokes law and allowed for the characterization of the forces created by motor proteins like Myosin, Dynein and Kinesin [22]–[25]. The use of beads instead of cellular material increased the timescales for trapping and made it easier to track the movement [10]. In recent publications the forces and movement of motor proteins have been characterized in vivo [26]–[28].

1.2 Force spectroscopy

1.2.1 Setup

The attachment of protein to beads also allowed for optical trapping to be applied in force spectroscopy. Force spectroscopy is performed by applying a force on a molecule, e.g. DNA or protein. A common setup for these optical tweezers consists of one bead trapped in a laser and a second bead held by a micropipette (figure 1) [29], [30]. A molecule is attached between the beads using antibodies or DNA linkers. The latter is easier to use and is generally applied nowadays [31]. Sometimes the non-trapped bead is replaced by a different object, for example an antibody covered coverslip that is on the bottom of the measuring compartment [32].
The dual optical trap setup, with both beads trapped by a laser, is also used and avoids the inaccuracy/drift by the micropipette [33]–[35].
There are multiple ways of exerting force on a tether in force spectroscopy. The most used are the 'force ramp' and 'constant force-feedback'. The force ramp is performed by pulling on the tether at a constant speed. The force increases exponentially and results in a force-extension curve as

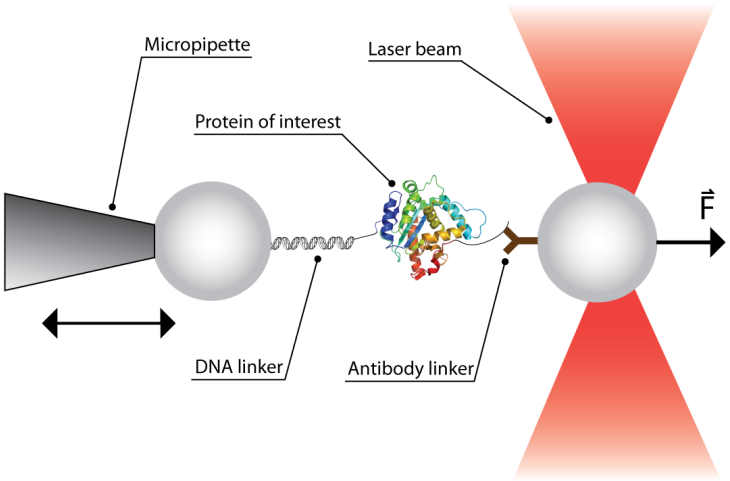

Figure 1. Optical tweezer setup
In this setup the protein of interest is attached between two beads by using either antibody linkers or DNA linkers. The beads are held in the optical trap and on the tip of a micropipette. The micropipette is used to pull the optical trapped bead out of the center of the laser beam which applies a force on the tether.
In a dual optical trap setup the laser beam is split and both beams are focused, creating two optical traps. The distance between the laser traps can be altered which is used to apply a force on the tether.

shown in figure 2. The force at which folding transitions occur is dependent on the pulling speed and is used to determine the kinetics of the folding transitions [29]. Also, the difference in tether length between these transitions can be determined by using the worm like chain (WLC) model. The model describes the force on the tether by the length of the tether (contour length), a measure for the flexibility of the tether (persistence length) and the extension of the tether, measured by the distance between the beads [29], [36], [37].

Constant force-feedback is performed by keeping a constant force or extension on the tether. While keeping the force on a tether constant, folding transitions can occur over time as shown in figure 3. The change in force due to the transitions can be corrected by changing the extension right after a transition [38] or the extension is kept constant while the force on the tether changes [39]. The latter is preferred because it avoids the need for correcting the force, which limits the observation of states with a low lifetime [40]–[42]. Optical tweezers are favorable for keeping a constant force due to their low trap stiffness. With a constant extension the force changes only slightly after folding transitions [34].

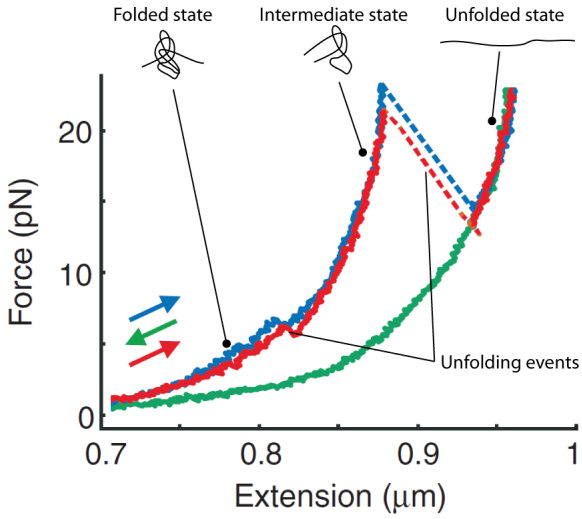

Figure 2. Force ramp experiment
The protein MBP is extended and unfolded using a force ramp. The blue trace is the initial stretching where two unfolding events can be distinguished. The green trace is the following release of force after which the protein is stretched again (red trace). The red trace shows similar characteristics as the first unfolding
Figure is reproduced from [95].

1.2.2 Characterization and unfolding of DNA and RNA

Characterizing the elasticity of DNA molecules has been one of the first applications of optical tweezers in force spectroscopy [43], [44]. Mechanically extending DNA molecules increased the force on the tether exponentially. The resulting curve was modeled using polymer models such as the freely jointed chain and WLC model, from which the latter is still used nowadays [36], [45], [46]. Single stranded DNA and RNA form molecular structures, e.g. hairpins, ribosomal components, whose unfolding can be observed and characterized with force spectroscopy [47], [48]. The interactions that make up (small) DNA/RNA structures are predictable and allows for the determination of sequence dependent kinetics and control over the folding landscape [49].

1.2.3 Unfolding of protein

Titin was used for the first force spectroscopy experiments on single proteins. Titin is a big muscle protein that contains ~300 domains and is responsible for building up a passive force while stretching a muscle. Next to optical tweezers [29] also Atomic Force Microscopy (AFM) was used to exert force on Titin [37]. In these experiments Titin was attached to a gold surface with the C-terminus while the AFM cantilever picked up the protein at a random location. With the subsequent bending of the cantilever the force on the protein between the surface and cantilever was measured (figure 4a).

The results for both methods have uncovered a fundamental difference in their setup. Where AFM is able to detect the unfolding of each individual domain, the optical tweezers show a continuous unfolding without single drops in force (figure 4). The cause for this difference is found in the stiffness of the setup. AFM is able to pull with a high force, but a small increase in extension also increases the force significantly. Optical tweezers on the other hand have a low stiffness, resulting in a small decrease in force when a single domain unfolds [50]. In the early 00s AFM has primarily been used for protein folding studies due to a relative easy setup [51]–[53]. However, the low stiffness made optical tweezers ideal for constant force-feedback, which has given a unique insight in protein folding studies [39], [54].

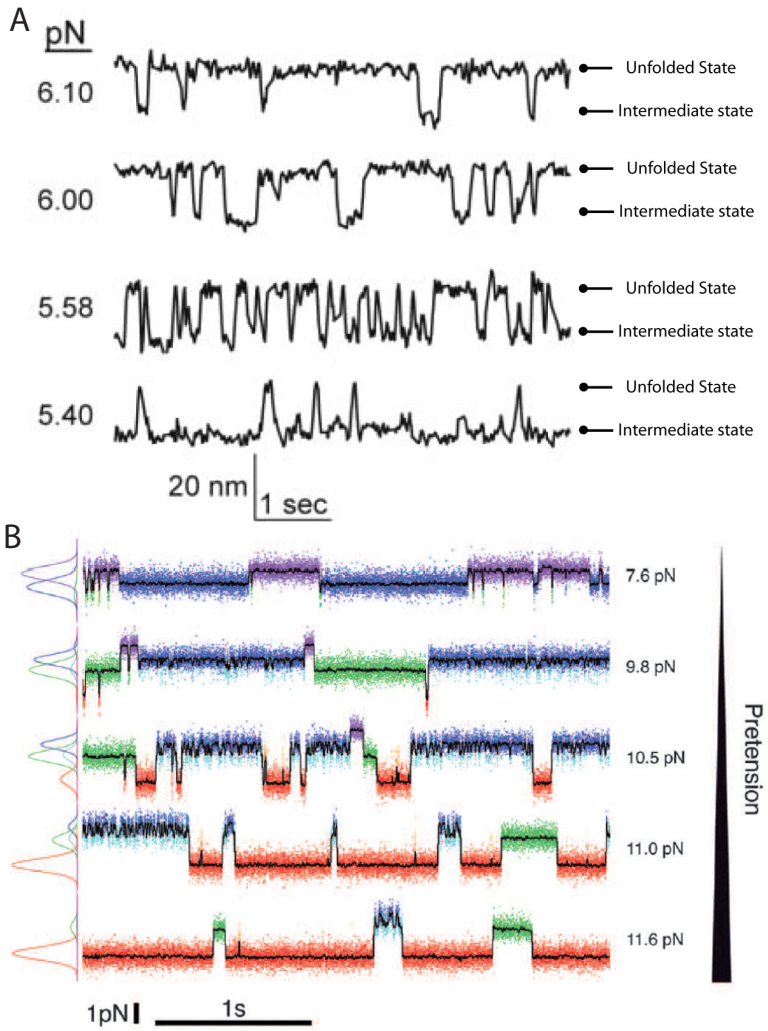

Figure 3. Constant force-feedback experiments
(A) The transition between the unfolded and the intermediate state of RNase H was observed in real time at different pretensions. The pretension is the force that is kept constant throughout the experiment and is shown on the left. At higher pretensions the unfolded state is mainly populated.
(B) The transitions between the 6 folding states of Calmodulin are followed in real time. The colors match the folding states in figure 5b. On the left the histograms for the occurance of each folding state is shown. With each transition the force changes, so the green folding state was chosen as the reference pretension.
The figures were reproduced from [39] and [54].

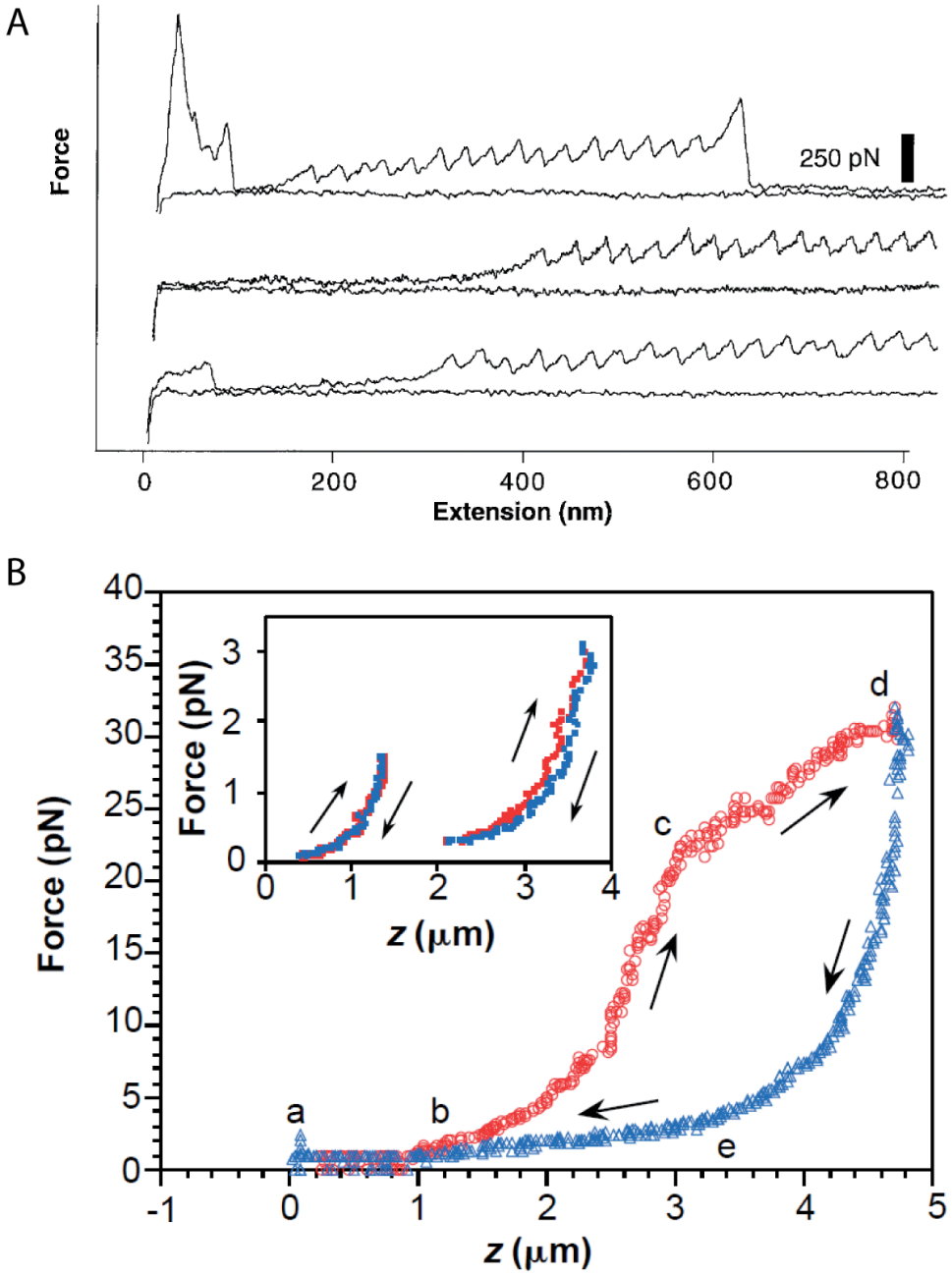

Figure 4. Extension of Titin using AFM and optical tweezers
(A) The three curves are seperate extensions of Titin. The 'shark tooth' pattern that is observed after 200 nm extension is the unfolding of single Titin domains. The black line under this pattern is the release of force. Each drop was analyzed with the WLC model and showed that the average increase in contour length is similar to the theoretical increase after unfolding. The different observations before the 200 nm extension are due to random attachment of the AFM tip to the protein.
(B) A single stretch (red circles) and release (blue triangles) curve of Titin is shown. Up to point c the the stretch curve shows WLC behaviour after which Titin begins to unfold. The release curve, which starts at point d, shows the behaviour of a WLC with a higher contour length, indicating that Titin is (partially) unfolded. Also, the stretch curves in which the force is released before point c overlap with the following release curves, indicating that no unfolding has occured yet (inset).
The figures are reproduced from [37] and [29].

Chapter 2

Determination of folding kinetics by unfolding protein with optical tweezers

2.1 Kinetics in protein folding

To visualize the protein folding process and its kinetics the Gibbs free energy plot is often used [55]. The simplest plot involves a folded state and an unfolded state which are divided by an energy barrier (figure 5a). In order to have a folding transition the barrier has to be overcome which is depicted by the energy difference ΔG^F for folding and ΔG^U for unfolding. The (relative) height of the folding states and the barrier can be determined using the rate at which the state transitions (k_u and k_f) occur, which is called the kinetics of the folding process [56]. The distance between the states on the x-axis is measured on an arbitrary reaction coordinate. For force spectroscopy the distance between the two ends of the protein is used, which has been confirmed as a reliable reaction coordinate [57].

When taking intermediate folding states into account the free energy plot becomes more complicated. An on-pathway intermediate, which is between the folded and unfolded state on the reaction coordinate, splits the activation energy barrier into two with the intermediate folding state between them. Visualizing an off-pathway folding state is more difficult. Often it is placed next to the unfolded state, because the protein has to be unfolded before folding into the native state. However, it is also possible that an off-pathway intermediate state is reached via an on-pathway intermediate state for which a 3-dimensinal representation of the folding landscape is needed to visualize all folding states (figure 5b).

As the unfolding of proteins often does not occur in observable timescales certain techniques are used to disrupt the folded protein in order to determine its folding landscape. For example, mutations, addition of detergent or denaturant, heat or pressure are used to (partially) unfold protein [58]–[60]. In the energy landscape this can be visualized by the lowering of the unfolded state energy level or the folding barrier, or raising the folded state energy level. Subsequently, the folding landscape in native conditions is determined by extrapolating the kinetics from the disrupted conditions [61].

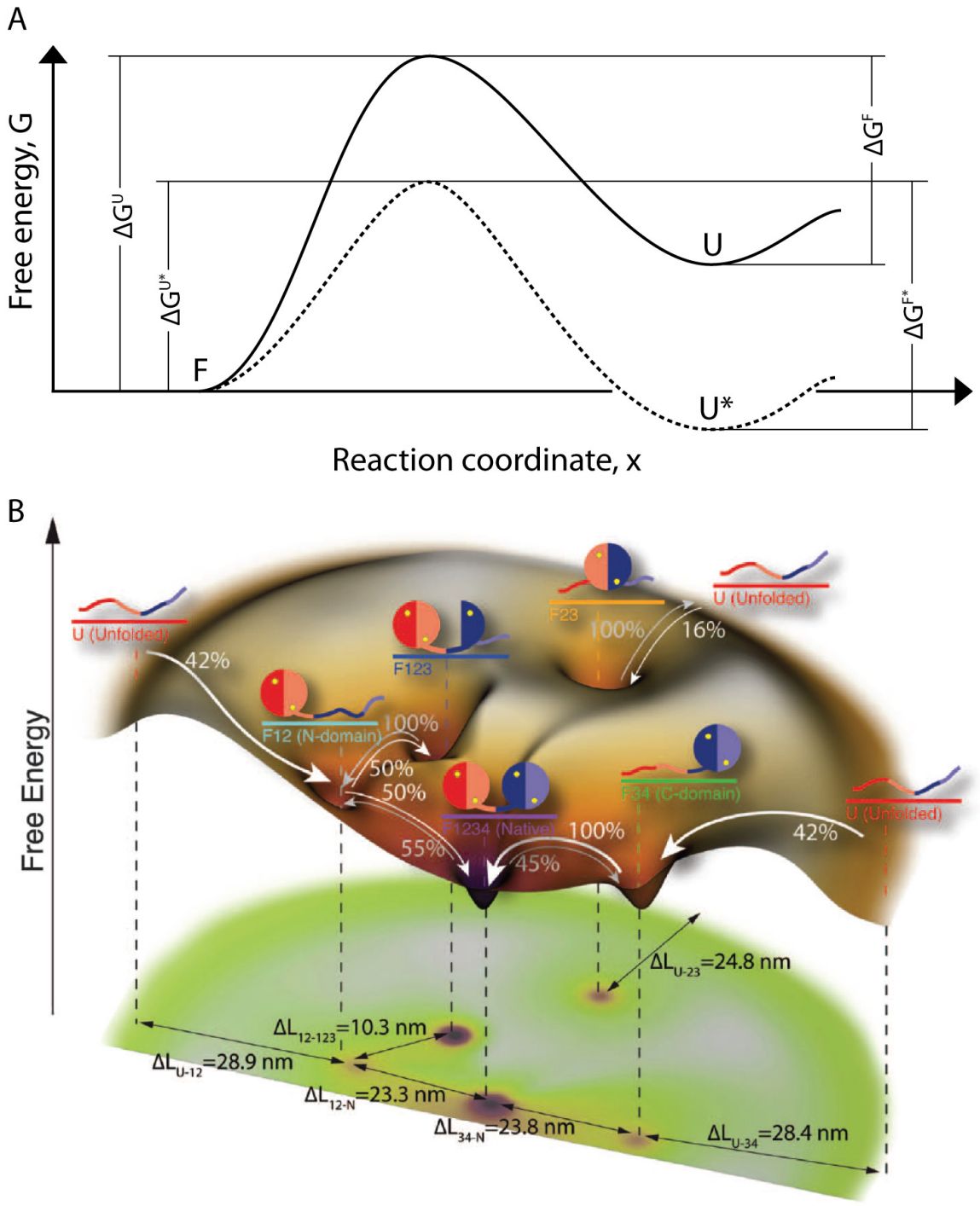

Figure 5. Energy landscapes of protein folding

(A) A schematic free energy landscape for a two-state folding protein. The heigth of the barrier between the folded (F) and unfolded (U) states are related the rate of folding and unfolding ($\Delta G \sim k^{-1}$). Under influence of force the landscape tilts around the folded state (dotted line) and changes the relative height of the folding barrier. The folding transition becomes less likely ($\Delta G^F < \Delta G^{F*}$) and the unfolding becomes more likely to happen ($\Delta G^U > \Delta G^{U*}$).

(B) The three dimensional energy landscape of Calmodulin in the absence of force as determined with optical tweezers using constant force-feedback. The folding pathway goes from the outside (the red unfolded states) to the center of the figure like a funnel. There are two misfolded states, F23 and F123, from which the latter is only reachable through the F12 intermediate state. The differences in contour length between the states are indicated by ΔL. The percentages give an indication of the kinetics from each state. Figure 2b was reproduced from [54].

2.2 Kinetics in single molecule force spectroscopy

In force spectroscopy, force is used to disrupt the fold of a protein. The influence of force on the energy landscape is best visualized in the 2-dimensional energy plot. Applying force on a protein tilts the entire plot around the folded state proportionally to the applied force (figure 5a) [52], [62]. The energy of the folding states and energy barrier decrease proportional to the reaction coordinate which increases the rate (or chance) of unfolding. At enough force the folding transitions occur within the timescale of a single experiment.

The measurement of single molecules in force spectroscopy provides a unique viewpoint of the protein folding process. Ensemble techniques like NMR, x-ray crystallography and CD-spectroscopy always look at multiple proteins which results in missing low populated folding states due to the averaging over all folding states [63], [64]. Single molecule experiments on the other hand observe the folding state of a single protein over time. Folding states that do not occur often or with low lifetime can be directly observed, although long measurement times are needed for rare events and the observable lifetime of a folding state is limited by the response time of the experimental setup [41], [65], [66].

For determining the free energy differences and kinetics for a folding energy landscape it is generally required for the system to be in equilibrium. In other words, the population of each state has to be constant to determine and extrapolate the folding rates. Ensemble studies are generally in equilibrium due to the long measurement times and the amount of molecules measured at a time. In single molecule studies on the other hand only one protein is observed at a time, which means that at each folding transition the whole system changes [67]. To still be able to use thermodynamics for force spectroscopy either the equilibrium conditions are approximated or the changes in the system are minimized, for example by using constant force feedback [41].

2.2.1 Non-equilibrium experiments

The force ramp is one of the most used techniques in force spectroscopy which is non-equilibrium due to the constant changing force. For the determination of the native folding landscape, the work done in the folding transitions or the folding and unfolding rate are used. The work done during folding transitions in a force ramp is related to the free energy difference as is stated by the fluctuation theorem [68]. However, with this theorem it is only possible to calculate the free energy from near-equilibrium conditions. With the derivation of Jarzynski's equality, which is based on the fluctuation theorem, the range of obtaining equilibrium

information from non-equilibrium experiments increased significantly [69], [70]. Nonetheless, multiple extensions of Jarzynski's equality have been developed to give an even more accurate approximation [68], [71]. Two of these extensions are Crook's fluctuation theorem (CFT) and the model of Hummer and Szabo [72]–[74]. Jarzynski's equality and these extensions have been verified using the folding of a RNA hairpin whose folding has been studied with ensemble methods [73], [75], [76].

The rate of unfolding in a force ramp experiment is determined by repeatedly measuring the force at which unfolding occurs. Due to the constantly increasing rate of unfolding a distribution of the unfolding force is observed. Additionally, the most likely force at which unfolding occurs is dependent on the pulling speed. A lower pulling speed gives more chance for the protein to unfold at a lower force. So for measuring the native unfolding rate a histogram of unfolding forces or a plot with average unfolding force versus pulling speed is created. Both can be fit using a derivative of the Bell equation (equation 1) [51], [77]–[81].

(1) $k_u = k_0 \, Exp[F\Delta x/k_B T]$

The bell equation describes the unfolding rate (k_u) as a function of force (F), which depends on the native unfolding rate (k_0) and the distance from the transition state (Δx). However, the application of this equation is limited. The distance from the transition state is assumed to be constant, while this is only the case in small force ranges (~1 pN) [41]. Additionally, experimental parameters such as trap stiffness, bead size and DNA handle length affect the unfolding rate which have to be approximated and added as a factor in equation 1 [41], [82].

2.2.2 (Near-) equilibrium experiments

Using constant force-feedback allows for the determination of folding kinetics in near-equilibrium conditions. Measuring for long periods of time reduced the force at which unfolding is observed significantly by giving the protein more time to unfold at lower forces. With the use of silica beads measurements can be as long as 45 minutes [54]. Subsequently, the refolding rate is higher than in a force ramp, which makes it possible to repeatedly observe unfolding and refolding during one measurement. For example, the transition between the intermediate and unfolded state of RNase H has been observed at multiple pretensions (figure 3a) [39]. From the resulting traces the time each state is populated and the amount of transitions were extracted. Using the statistics of a 2-state system, the free energy difference of intermediate folding and unfolding was determined as a function of force [82], [83].

For the analysis of more complex folding landscapes the Hidden Markov Method (HMM) is used. The HMM is a mathematical model which describes a system with a number of states and probabilities for state transitions [84], [85]. It was used for the characterization of constant force traces observed for Calmodulin, which folds in six distinct states (figure 3b) [54]. Despite having three states with similar contour lengths the HMM was able to distinguish these folding states by their differences in lifetime [86], [87]. The determination of a folding landscape using the HMM data has been well described in the supplementary material of [54]. An extensive background and tutorial off the HMM has been described in [88].

Chapter 3

Application of optical tweezers in recent publications

In the last decade optical tweezers have been used a lot in protein folding studies. In this chapter several publications in which the optical tweezers are used will be highlighted. We will show how a different sample preparation and addition of ligands or substrates are used in protein folding studies and how the forces applied by molecular machinery such as the AAA+ protease complex, the von Willebrand Factor complex and the ribosome are characterized.

3.1 Preparation of the protein tether

The canonical approach for tether preparation is by connecting one or multiple proteins through the N- and C-termini. However, other tether designs have also been used to obtain insight into the folding process.

The SNARE complex is responsible for the docking and fusion of membranes in vesicle transport. Most proteins in the complex have trans-membrane segments, which makes it impossible to use in force spectroscopy due to their solubility. By expressing only the soluble parts of the complex and covalently connecting them through disulfide bonds, the unfolding and refolding of the concatenated complex was observed repeatedly. This tether design made it possible to observe and characterize the intermediate folding states that make up the docking and fusion process [89].

The observation of the ribosomal effect on nascent protein folding is difficult because most unfolding methods also affect the ribosome. However, by creating a tether that contains the ribosome as well as a protein whose expression is stopped before release, the protein folding could be observed by pulling on the ribosome and the protein. The ribosome was unaffected by the forces used in the experiment. Using linkers of varying size between the ribosome and protein it was shown that the ribosome does not affect the unfolding, but slows down the refolding as the protein is closer to the ribosome [90].

The addition of cytein residues as attachment points for beads allowed for custom force anchors. These anchors can be put throughout a protein, provided the protein lacks cystein residues on the surface of its structure or a cystein-less or -free construct can be engineered. Subsequently, the force axis on the protein is shifted which results in a change in the measurements [91]. For example, it takes more force to unfold a double beta sheet by pulling it from opposite ends instead of pulling it from the same side and 'unzipping' it [92].

The changing of the force axis has made it possible to calculate distance restraints in the folded protein. The distance restraints were determined by comparing the increase in countour length after unfolding with the theoretical distance between the force achors in the unfolded protein. The difference between the two is the distance between the force anchors in the folded protein. The distance restraints can be used to determine protein structures that are difficult to study with ensemble studies, for example intermediate and misfolded states [93].
Furthermore, changing the force axi on T4 lysozyme has shown the folding cooperativity between its two domains. The folding cooperativity comes from the C-terminal domain, which is discontinuous. Its most C-terminal alpha helix is expressed at the N-terminus. By repeatedly unfolding the N-terminal domain and applying CFT, the free energy difference of unfolding was determined. The free energy that was found is similar to the unfolding of the whole protein as observed in ensemble studies, indicating that by unfolding one domain the whole protein is unfolded. This finding was confirmed by making a circular permutation of T4 Lysozyme, in which the N-terminal alpha helix was expressed at the C-terminus, creating two continuous domains. The free energy of unfolding of the N-terminal domain in this construct was reduced significantly and corresponded well with ensemble studies that unfolded only the N-terminal domain [94].

3.2 Protein folding process after addition or removal of chaperones and metal ions.
Changing the solvent of a protein is one of the main tools that is used in folding studies. For example, ions, small soluble molecules or other proteins are added to observe their effect on the folding process of the protein in question. This has also been applied in combination with optical tweezers as the effect of added chaperones or calcium was observed.

The still largely unknown mechanism of chaperone assisted protein folding has been studied at the single molecule level using optical tweezers. The maltose binding protein (MBP) was repeatedly unfolded and refolded in the presence of the chaperones SecB [95] or trigger factor (TF) [96]. Tethers containing either one or four copies of MBP were used as the MBP multimer has a high tendency to misfold or aggregate instead of refolding.
The experiments with SecB revealed that the chaperone keeps MBP unfolded after unfolding. The unfolding of both the single and multimer tether did not change in the presence of SecB. However, no folded MBP was observed after it was allowed to refold. Additionally, the misfolding of the multimer did not occur. Furthermore, the first step in the two-step unfolding of MBP was shown to be unaffected by SecB, which indicated that the chaperone only binds the unfolded core of MBP [95].

In the presence of the chaperone TF the observations were completely different. Instead of unfolding MBP with one intermediate folding state, at least four distinct intermediate states have been observed which were characterized by their contour length. Also the force at which the protein is completely unfolded is higher with TF present which indicated that TF probably binds MBP and prevents unfolding. With a binding assay it was shown that only partially folded states bound TF so the binding only occurs during the unfolding. Additionally, the tendency for the MBP multimer to misfold was reduced significantly in the presence of TF [96].

Metal ions are part of many protein structures. They are encapsulated by short motifs and often modulate structural features and/or enzymatic activity [97]. Consequently, they are very important for the correct folding of these proteins. The unfolding and refolding of the protein Calmodulin [98] and the A2 domain of the von Willebrand Factor (vWF) [99] in the absence of calcium has been observed with optical tweezers. In both cases the stability of the folded state was reduced, as was observed by a lowered unfolding force and refolding rate. Additionally the intermediate folding state of the vWF protein is hardly observed, making the folding process an all-or-nothing process [99]. In the case of Calmodulin, only the N-terminal domain was able to fold. These findings indicate that folding still occurs, but is more precise, faster and the structure is more stable with calcium ions present [98].

3.3 Characterization of forces in cellular processes

3.3.1 Ribosome

During protein translation the ribosome may encounter a piece of messenger RNA that has folded into a three dimensional structure. The ribosome is able to unfold these structures, but the exact mechanism remained elusive. With the optical tweezers setup the unfolding of a RNA hairpin was followed in real time by attaching a RNA hairpin between two beads after which ribosomes were added [100]. The contour length of the RNA increased as the ribosome reads the RNA and unfolds the hairpin. The steps in which the unfolding occurred could be quantified by triplets of base pairs or single codons. Additionally, the ribosome often pauses between the steps for short periods of time [100]. Furthermore, the force that is exerted on the hairpin during the measurements affected the translation speed. A higher force helps the ribosome in unfolding the hairpin and subsequently increases the translation speed. Also, more guanine and cytosine in the hairpin decreased the translation speed and increased the force at which the hairpin unfolds without the ribosome [101].

Quantitative analysis of these data showed that there are two processes with which the ribosome unfolds the RNA hairpin [101]. First is the application of a direct force that unzips the hairpin. This ensures a basal unfolding speed and originates from the movement of the ribosome during translation. Second is the destabilization of the hairpin, which reduces the force that is needed to unfold the hairpin. The nature of this process is still unknown, but the characterization of the ribosomal protein S1, which is able to destabilize RNA hairpins [102], could indicate that this protein is involved in this process.

3.3.2 ClpXP protease complex

The ClpXP complex is responsible for the complete degradation of proteins and consists of two parts. ClpX is a doughnut shaped protein that recognizes proteins that are tagged for degradation, unfolds them and pulls them through its center pore. Subsequently, the barrel shaped ClpP degrades the protein. The translocation and unfolding of the substrate was followed directly using optical tweezers. The ClpXP complex was attached to one bead while a substrate was attached to the other bead [103].

To characterize the force that the complex generates, a countering force was applied with the optical tweezers. The translocation speed gradually decreased with increasing force until it stalled at ~20 pN, indicating that 20 pN is the force that the ClpX can generate. This is enough to unfold most proteins, especially when considering the low loading rate, which was estimated to be 0.15 pN/s. Furthermore, the step size of translocation was determined to be multitudes of 1 nm. Analysis of the ClpX structure showed that a single stroke of a ClpX monomer could move a protein for ~ 1 nm. So the force generated by the ATP hydrolysis in ClpX was concluded to be the main contribution to the unfolding. However, allosteric effects are not excluded [104].

3.3.3 Blood clotting

Blood clotting is an intricate process which is preceded by multiple protein reactions that allow for specific and local clotting. The localization of the clotting in blood vessels is performed by vWF. This protein is expressed and secreted into the blood as a concatemer with a broad size distribution, where it binds to collagen that is exposed when a blood vessel is damaged. Due to its globular fold the vWF concatemer is inactive until it is stretched by the shear forces in the blood stream. This exposes binding sites for enzymes that initiate blood clotting [105]. To regulate the blood clotting signal and prevent non-specific clot formation the concatemer can be cleaved at the A2 domain, which reduces the size and subsequently the shear force on the

protein. However, the cleavage site is buried within the A2 domain, so the domain has to be unfolded before cleavage can take place. It was estimated that a concatemer of about 200 vWF monomers is enough to unfold the A2 domain when it is bound to a damaged blood vessel [106]. Additionally, the direct observation of the unfolding transitions of VWF allowed for the characterization of mutations that affect the blood clotting, creating a platform for identifying blood clotting diseases at molecular level and subsequent drug design [80], [107].

References

1. J. P. Barton, D. R. Alexander, S. A. Schaub, Theoretical determination of net radiation force and torque for a spherical particle illuminated by a focused laser beam, J. Appl. Phys. 66, 4594–4602 (1989).
2. A. Ashkin, Acceleration and trapping of particles by radiation pressure, Phys. Rev. Lett. 24, 156–159 (1970).
3. K. C. Neuman, S. M. Block, Optical trapping, Rev. Sci. Instrum. 75, 2787 (2004).
4. A. Ashkin, J. M. Dziedzic, J. E. Bjorkholm, S. Chu, Observation of a single-beam gradient force optical trap for dielectric particles, Opt. Lett. 11, 288–290 (1986).
5. A. Ashkin, Forces of a single-beam gradient laser trap on a dielectric sphere in the ray optics regime, Biophys. J. 61, 569–582 (1992).
6. A. Ashkin, J. P. Gordon, Stability of radiation-pressure particle traps: an optical Earnshaw theorem, Opt. Lett. 8, 511–513 (1983).
7. J. A. Lock, Calculation of the Radiation Trapping Force for Laser Tweezers by Use of Generalized Lorenz-Mie Theory. II. On-Axis Trapping Force, Appl. Opt. 43, 2545–2554 (2004).
8. T. A. Nieminen, G. Knöner, N. R. Heckenberg, H. Rubinsztein-Dunlop, in Methods in Cell Biology, (Academic Press, 2007), vol. 82, pp. 207–236.
9. R. W. Bowman, M. J. Padgett, Optical trapping and binding, Rep. Prog. Phys. 76, 026401 (2013).
10. S. M. Block, Making light work with optical tweezers, Nature 360, 493–495 (1992).
11. F. M. J. Cozijn et al., Laser cooling of beryllium ions using a frequency-doubled 626 nm diode laser, Opt. Lett. 38, 2370 (2013).
12. M. Morrissey et al., Spectroscopy, Manipulation and Trapping of Neutral Atoms, Molecules, and Other Particles Using Optical Nanofibers: A Review, Sensors 13, 10449–10481 (2013).
13. V. S. Letokhov, V. G. Minogin, Laser radiation pressure on free atoms, Phys. Rep. 73, 1–65 (1981).
14. Y. Chang, L. Hsu, S. Chi, Optical trapping of a spherically symmetric sphere in the ray-optics regime: a model for optical tweezers upon cells, Appl. Opt. 45, 3885–3892 (2006).
15. S. M. Block, D. F. Blair, H. C. Berg, Compliance of bacterial flagella measured with optical tweezers, Nature 338, 514–518 (1989).
16. A. Ashkin, K. Schütze, J. M. Dziedzic, U. Euteneuer, M. Schliwa, Force generation of organelle transport measured in vivo by an infrared laser trap, Nature 348, 346–348 (1990).
17. N. Hyun et al., Effects of viscosity on sperm motility studied with optical tweezers, J. Biomed. Opt. 17, 0250051–0250056 (2012).
18. M.-C. Zhong, X.-B. Wei, J.-H. Zhou, Z.-Q. Wang, Y.-M. Li, Trapping red blood cells in living animals using optical tweezers, Nat. Commun. 4, 1768 (2013).
19. D. J. Stevenson, F. Gunn-Moore, K. Dholakia, Light forces the pace: optical manipulation for biophotonics, J. Biomed. Opt. 15, 041503–041503–21 (2010).
20. S. M. Block, L. S. B. Goldstein, B. J. Schnapp, Bead movement by single kinesin molecules studied with optical tweezers, Nature 348, 348–352 (1990).
21. K. Svoboda, C. F. Schmidt, B. J. Schnapp, S. M. Block, Direct observation of kinesin stepping by optical trapping interferometry, Nature 365, 721–727 (1993).
22. J. T. Finer, R. M. Simmons, J. A. Spudich, Single myosin molecule mechanics: piconewton forces and nanometre steps, Nature 368, 113–119 (1994).
23. K. Svoboda, S. M. Block, Force and velocity measured for single kinesin molecules, Cell 77, 773–784 (1994).
24. K. Visscher, M. J. Schnitzer, S. M. Block, Single kinesin molecules studied with a molecular force clamp, Nature 400, 184–189 (1999).
25. A. D. Mehta, M. Rief, J. A. Spudich, D. A. Smith, R. M. Simmons, Single-Molecule Biomechanics with Optical Methods, Science 283, 1689–1695 (1999).
26. C. Veigel, C. F. Schmidt, Moving into the cell: single-molecule studies of molecular motors in complex environments, Nat. Rev. Mol. Cell Biol. 12, 163–176 (2011).
27. A. K. Rai, A. Rai, A. J. Ramaiya, R. Jha, R. Mallik, Molecular Adaptations Allow Dynein to Generate Large Collective Forces inside Cells, Cell 152, 172–182 (2013).
28. L. B. Oddershede, Force probing of individual molecules inside the living cell is now a reality, Nat. Chem. Biol. 8, 879–886 (2012).
29. M. S. Z. Kellermayer, S. B. Smith, H. L. Granzier, C. Bustamante, Folding-Unfolding Transitions in Single Titin Molecules Characterized with Laser Tweezers, Science 276, 1109–1112 (1997).
30. M. S. Z. Kellermayer, S. B. Smith, C. Bustamante, H. L. Granzier, Complete Unfolding of the Titin Molecule under External Force, J. Struct. Biol. 122, 197–205 (1998).
31. C. Cecconi, E. A. Shank, F. W. Dahlquist, S. Marqusee, C. Bustamante, Protein-DNA chimeras for single molecule mechanical folding studies with the optical tweezers, Eur. Biophys. J. 37, 729–738 (2008).
32. L. Tskhovrebova, J. Trinick, J. Sleep, R. Simmons, Elasticity and unfolding of single molecules of the giant muscle protein titin, Nature , 308–12 (1997).
33. J. R. Moffitt, Y. R. Chemla, D. Izhaky, C. Bustamante, Differential detection of dual traps improves the spatial resolution of optical tweezers, Proc. Natl. Acad. Sci. 103, 9006–9011 (2006).
34. J. C. M. Gebhardt, T. Bornschlogl, M. Rief, Full distance-resolved folding energy landscape of one single protein molecule, Proc. Natl. Acad. Sci. 107, 2013–2018 (2010).

35. M. C. Leake, D. Wilson, B. Bullard, R. M. Simmons, The elasticity of single kettin molecules using a two-bead laser-tweezers assay, FEBS Lett. 535, 55–60 (2003).
36. M. Fixman, Polymer conformational statistics. III. Modified Gaussian models of stiff chains, J. Chem. Phys. 58, 1564 (1973).
37. M. Rief, M. Gautel, F. Oesterhelt, J. M. Fernandez, H. E. Gaub, Reversible Unfolding of Individual Titin Immunoglobulin Domains by AFM, Science 276, 1109–1112 (1997).
38. M. Schlierf, H. Li, J. M. Fernandez, The unfolding kinetics of ubiquitin captured with single-molecule force-clamp techniques, Proc. Natl. Acad. Sci. U. S. A. 101, 7299–7304 (2004).
39. C. Cecconi, E. A. Shank, C. Bustamante, S. Marqusee, Direct Observation of the Three-State Folding of a Single Protein Molecule, Science 309, 2057–2060 (2005).
40. J. P. Junker, F. Ziegler, M. Rief, Ligand-Dependent Equilibrium Fluctuations of Single Calmodulin Molecules, Science 323, 633–637 (2009).
41. P. J. Elms, J. D. Chodera, C. J. Bustamante, S. Marqusee, Limitations of Constant-Force-Feedback Experiments, Biophys. J. 103, 1490–1499 (2012).
42. W. J. Greenleaf, M. T. Woodside, E. A. Abbondanzieri, S. M. Block, Passive All-Optical Force Clamp for High-Resolution Laser Trapping, Phys. Rev. Lett. 95, 208102 (2005).
43. J. F. Marko, E. D. Siggia, Stretching dna, Macromolecules 28, 8759–8770 (1995).
44. C. Bustamante, J. Marko, E. Siggia, S. Smith, Entropic elasticity of lambda-phage DNA, Science 265, 1599–1600 (1994).
45. C. Bouchiat et al., Estimating the persistence length of a worm-like chain molecule from force-extension measurements, Biophys. J. 76, 409–413 (1999).
46. Z. Xi, Y. Gao, G. Sirinakis, H. Guo, Y. Zhang, Single-molecule observation of helix staggering, sliding, and coiled coil misfolding, Proc. Natl. Acad. Sci. 109, 5711–5716 (2012).
47. J. Liphardt, B. Onoa, S. B. Smith, I. Tinoco, C. Bustamante, Reversible Unfolding of Single RNA Molecules by Mechanical Force, Science 292, 733–737 (2001).
48. Y. Cui, C. Bustamante, Pulling a single chromatin fiber reveals the forces that maintain its higher-order structure, Proc. Natl. Acad. Sci. U. S. A. 97, 127–132 (2000).
49. M. T. Woodside et al., Direct Measurement of the Full, Sequence-Dependent Folding Landscape of a Nucleic Acid, Science 314, 1001–1004 (2006).
50. A. D. Mehta, K. A. Pullen, J. A. Spudich, Single molecule biochemistry using optical tweezers, FEBS Lett. (1998).
51. P. M. Williams et al., Hidden complexity in the mechanical properties of titin, Nature 422, 446–449 (2003).
52. R. Merkel, P. Nassoy, A. Leung, K. Ritchie, E. Evans, Energy landscapes of receptor–ligand bonds explored with dynamic force spectroscopy, Nature 397, 50–53 (1999).
53. F. Oesterhelt et al., Unfolding Pathways of Individual Bacteriorhodopsins, Science 288, 143–146 (2000).
54. J. Stigler, F. Ziegler, A. Gieseke, J. C. M. Gebhardt, M. Rief, The Complex Folding Network of Single Calmodulin Molecules, Science 334, 512–516 (2011).
55. J. N. Onuchic, Z. Luthey-Schulten, P. G. Wolynes, Theory of protein folding: the energy landscape perspective, Annu. Rev. Phys. Chem. 48, 545–600 (1997).
56. J. D. Bryngelson, P. G. Wolynes, Intermediates and barrier crossing in a random energy model (with applications to protein folding), J. Phys. Chem. 93, 6902–6915 (1989).
57. O. K. Dudko, T. G. W. Graham, R. B. Best, Locating the Barrier for Folding of Single Molecules under an External Force, Phys. Rev. Lett. 107, 208301 (2011).
58. M. Zolkiewski, M. J. Redowicz, E. D. Korn, A. Ginsburg, Thermal unfolding of Acanthamoeba myosin II and skeletal muscle myosin, Biophys. Chem. 59, 365–371 (1996).
59. D. I. Levitsky, A. V. Pivovarova, V. V. Mikhailova, O. P. Nikolaeva, Thermal unfolding and aggregation of actin, FEBS J. 275, 4280–4295 (2008).
60. F. Meersman, L. Smeller, K. Heremans, Protein stability and dynamics in the pressure-temperature plane, Biochim. Biophys. Acta 1764, 346–354 (2006).
61. T. O. Street, N. Courtemanche, D. Barrick, in Methods in Cell Biology, Biophysical Tools for Biologists, Volume One: In Vitro Techniques. I. Dr. John J. Correia and Dr. H. William Detrich, Ed. (Academic Press, 2008), vol. Volume 84, pp. 295–325.
62. E. Evans, Probing the Relation Between Force—Lifetime—and Chemistry in Single Molecular Bonds, Annu. Rev. Biophys. Biomol. Struct. 30, 105–128 (2001).
63. F. Ritort, Single-molecule experiments in biological physics: methods and applications, J. Phys. Condens. Matter 18, R531–R583 (2006).
64. A. Borgia, P. M. Williams, J. Clarke, Single-Molecule Studies of Protein Folding, Annu. Rev. Biochem. 77, 101–125 (2008).
65. F. Ritort, C. Bustamante, I. Tinoco, A two-state kinetic model for the unfolding of single molecules by mechanical force, Proc. Natl. Acad. Sci. 99, 13544–13548 (2002).
66. H. Yu et al., Direct observation of multiple misfolding pathways in a single prion protein molecule, Proc. Natl. Acad. Sci. 109, 5283–5288 (2012).
67. I. Tinoco Jr, C. Bustamante, The effect of force on thermodynamics and kinetics of single molecule reactions, Biophys. Chem. 101, 513–533 (2002).
68. D. J. Evans, D. J. Searles, The Fluctuation Theorem, Adv. Phys. 51, 1529–1585 (2002).
69. C. Jarzynski, Equilibrium free-energy differences from nonequilibrium measurements: A master-equation approach, Phys. Rev. E 56, 5018–5035 (1997).
70. C. Jarzynski, Nonequilibrium Equality for Free Energy Differences, Phys. Rev. Lett. 78, 2690–2693 (1997).

71. G. E. Crooks, Entropy production fluctuation theorem and the nonequilibrium work relation for free energy differences, Phys. Rev. E 60, 2721–2726 (1999).
72. G. Hummer, A. Szabo, Kinetics from Nonequilibrium Single-Molecule Pulling Experiments, Biophys. J. 85, 5–15 (2003).
73. G. Hummer, A. Szabo, Free Energy Surfaces from Single-Molecule Force Spectroscopy, Acc. Chem. Res. 38, 504–513 (2005).
74. O. K. Dudko, G. Hummer, A. Szabo, Intrinsic Rates and Activation Free Energies from Single-Molecule Pulling Experiments, Phys. Rev. Lett. 96, 108101 (2006).
75. J. Liphardt, S. Dumont, S. B. Smith, I. Tinoco, C. Bustamante, Equilibrium Information from Nonequilibrium Measurements in an Experimental Test of Jarzynski's Equality, Science 296, 1832–1835 (2002).
76. D. Collin et al., Verification of the Crooks fluctuation theorem and recovery of RNA folding free energies, Nature 437, 231–234 (2005).
77. G. Bell, Models for the specific adhesion of cells to cells, Science 200, 618–627 (1978).
78. J. P. Junker, M. Rief, Evidence for a Broad Transition-State Ensemble in Calmodulin Folding from Single-Molecule Force Spectroscopy, Angew. Chem. Int. Ed. 49, 3306–3309 (2010).
79. O. K. Dudko, G. Hummer, A. Szabo, Theory, analysis, and interpretation of single-molecule force spectroscopy experiments, Proc. Natl. Acad. Sci. U. S. A. 105, 15755–15760 (2008).
80. M. Arya et al., Dynamic Force Spectroscopy of Glycoprotein Ib-IX and von Willebrand Factor, Biophys. J. 88, 4391–4401 (2005).
81. Q. Peng, H. Li, Atomic force microscopy reveals parallel mechanical unfolding pathways of T4 lysozyme: Evidence for a kinetic partitioning mechanism, Proc. Natl. Acad. Sci. 105, 1885–1890 (2008).
82. G. Diezemann, A. Janshoff, Dynamic force spectroscopy: Analysis of reversible bond-breaking dynamics, J. Chem. Phys. 129, 084904 (2008).
83. G. Diezemann, A. Janshoff, Force-clamp spectroscopy of reversible bond breakage, J. Chem. Phys. 130, 041101 (2009).
84. L. E. Baum, T. Petrie, Statistical Inference for Probabilistic Functions of Finite State Markov Chains, Ann. Math. Stat. 37, 1554–1563 (1966).
85. S. R. Eddy, What is a hidden Markov model?, Nat. Biotechnol. 22, 1315–1316 (2004).
86. J. D. Chodera et al., Bayesian hidden Markov model analysis of single-molecule force spectroscopy: Characterizing kinetics under measurement uncertainty, arXiv:1108.1430 (2011) (available at http://arxiv.org/abs/1108.1430).
87. J. Stigler, M. Rief, Hidden Markov Analysis of Trajectories in Single-Molecule Experiments and the Effects of Missed Events, ChemPhysChem 13, 1079–1086 (2012).
88. L. R. Rabiner, A tutorial on hidden Markov models and selected applications in speech recognition, Proc. IEEE 77, 257–286 (1989).
89. Y. Gao et al., Single Reconstituted Neuronal SNARE Complexes Zipper in Three Distinct Stages, Science 337, 1340–1343 (2012).
90. C. M. Kaiser, D. H. Goldman, J. D. Chodera, I. Tinoco, C. Bustamante, The Ribosome Modulates Nascent Protein Folding, Science 334, 1723–1727 (2011).
91. M. Carrion-Vazquez et al., The mechanical stability of ubiquitin is linkage dependent, Nat. Struct. Biol. 10, 738–743 (2003).
92. D. J. Brockwell et al., Pulling geometry defines the mechanical resistance of a β-sheet protein, Nat. Struct. Mol. Biol. 10, 731–737 (2003).
93. H. Dietz, M. Rief, Protein structure by mechanical triangulation, Proc. Natl. Acad. Sci. U. S. A. 103, 1244–1247 (2006).
94. E. A. Shank, C. Cecconi, J. W. Dill, S. Marqusee, C. Bustamante, The folding cooperativity of a protein is controlled by its chain topology, Nature 465, 637–640 (2010).
95. P. Bechtluft et al., Direct Observation of Chaperone-Induced Changes in a Protein Folding Pathway, Science 318, 1458–1461 (2007).
96. A. Mashaghi et al., Reshaping of the conformational search of a protein by the chaperone trigger factor, Nature 500, 98–101 (2013).
97. A. Lewit-Bentley, S. Réty, EF-hand calcium-binding proteins, Curr. Opin. Struct. Biol. 10, 637–643 (2000).
98. J. Stigler, M. Rief, Calcium-dependent folding of single calmodulin molecules, Proc. Natl. Acad. Sci. 109, 17814–17819 (2012).
99. A. J. Jakobi, A. Mashaghi, S. J. Tans, E. G. Huizinga, Calcium modulates force sensing by the von Willebrand factor A2 domain, Nat. Commun. 2, 385 (2011).
100. J.-D. Wen et al., Following translation by single ribosomes one codon at a time, Nature 452, 598–603 (2008).
101. X. Qu et al., The ribosome uses two active mechanisms to unwind messenger RNA during translation, Nature 475, 118–121 (2011).
102. X. Qu, L. Lancaster, H. F. Noller, C. Bustamante, I. Tinoco, Ribosomal protein S1 unwinds double-stranded RNA in multiple steps, Proc. Natl. Acad. Sci. U. S. A. 109, 14458–14463 (2012).
103. M.-E. Aubin-Tam, A. O. Olivares, R. T. Sauer, T. A. Baker, M. J. Lang, Single-Molecule Protein Unfolding and Translocation by an ATP-Fueled Proteolytic Machine, Cell 145, 257–267 (2011).
104. R. A. Maillard et al., ClpX(P) Generates Mechanical Force to Unfold and Translocate Its Protein Substrates, Cell 145, 459–469 (2011).
105. J. Ying, Y. Ling, L. A. Westfield, J. E. Sadler, J.-Y. Shao, Unfolding the A2 Domain of Von Willebrand Factor with the Optical Trap, Biophys. J. 98, 1685–1693 (2010).
106. X. Zhang, K. Halvorsen, C.-Z. Zhang, W. P. Wong, T. A. Springer, Mechanoenzymatic Cleavage of the Ultralarge Vascular Protein von Willebrand Factor, Science 324, 1330–1334 (2009).
107. A. J. Xu, T. A. Springer, Mechanisms by which von Willebrand Disease Mutations Destabilize the A2 Domain, J. Biol. Chem. 288, 6317–6324 (2013).